Supplementary information

A Microwave-Heat-Thermoelectric Cascade Platform for Dynamic Therapy Based on Schottky-Engineered Bismuth Telluride Nanosheets

Changsong Tian[a,b], Guochen Xu[a,b], Zengzhen Chen[a], Qiong Wu[a], Longfei Tan[a], Changhui Fu[a], Xiangling Ren[a], Xianwei Meng[a,*]

[a]*State Key Laboratory of Cryogenic Science and Technology, Technical Institute of Physics and Chemistry, Chinese Academy of Sciences; Laboratory of Controllable Preparation and Application of Nanomaterials, Technical Institute of Physics and Chemistry, Chinese Academy of Sciences, Beijing 100190, China*

[b]*University of Chinese Academy of Sciences, Beijing 100049, P. R. China*

**Corresponding authors. Tel.: 86-010-82543477*

E-mail: mengxw@mail.ipc.ac.cn (X.W. Meng)

Experiment

Reagents

$BiCl_3$ (98%), Na_2TeO_3 (99.9%), PVP (Mw ≈58000), Ethylene Glycol (EG, 99%), Bovine Serum Albumin (BSA, 96%), Glutathione (GSH, 98%), 5,5'-Dithiobis-(2-nitrobenzoic acid) (DTNB, 99%), 2, 3-bis (2- methoxy-4-nitro-5-sulfophehyl)−2H-tetrazolium-5-carboxanilide (XTT, 90%) were purchased from Shanghai Maclin Biochemical Technology Co., Ltd. Ethylenediaminetetraacetic acid disodium salt (EDTA, ≥99%) was obtained from the Guangdong Engineering Research Center for Fine Chemicals. $NaBH_4$ (98%) was purchased from Sinopharm Chemical Reagent Co., Ltd. $HAuCl_4$ was purchased from Beijing J&K Scientific Ltd. DCFH-DA, Calcein-AM/PI, JC-1 assay kit were purchased from Beyotime Biotechnology Co., Ltd.

Characterizations

The morphology of BT and BTA was characterized by Transmission Electron Microscope (TEM, HT-7700, Japan). Elements distribution and lattice interplanar spacing were characterized by high-resolution transmission electron microscope (Hitachi JEM-2100, Japan), Digital micrograph was used to measure the interplanar spacing. The elemental valence states and valence band positions were analyzed using X-ray photoelectron spectroscopy (XPS, Thermo Scientific K-Alpha, USA). Crystal information of material was analyzed by X-ray diffractometer (XRD, Bruker, Germany). The spectral information of the material was analyzed using a UV-VIS-NIR spectrophotometer (Cary 7000, Agilent, USA) and Raman imaging system (inVia Qontor, Renishaw, UK). Functional groups of materials were characterized by A Fourier transform infrared spectrometer (FTIR, Excalibur 3100, Varian, USA.). Fluorescence intensity was tested by fluorescence spectrometer (Cary Eclipse, Varian Technologies, USA.). Transient adsorption (TA) was analyzed by Ultrafast Transient Absorption and Two-Photon Spectroscopy System (Vitara-Legend Elite-Helios, Ultrafast, US). The electrochemical properties were characterized using an electrochemical workstation (CHI660E, China). •OH was detected by Electron

Paramagnetic Resonance Spectrometer (EPR, E500, Bruker BioSpin GmbH, Germany).

Synthesis of BTAB

Synthesis of Bi_2Te_3 (BT): 150 mg Na_2TeO_3, 156 mg $BiCl_3$, 200 mg PVP, 300 mg NaOH and 558 mg EDTA were dissolved in 24 mL EG. The mixture then reacted at 200 °C for 6 h. The precipitate was collected and washed by ethanol, and then dispersed in ethanol for storage.

Synthesis of Bi_2Te_3-Au (BTA): 12 mg BT was dispersed in 10 mL ethanol, then 40 μL $HAuCl_4$ (10 wt.%) was added. After stirring for 20 min, 0.5 mg $NaBH_4$ was added and reacted for 1 h at room temperature. The precipitate was washed by ethanol then dispersed in enthanol for storage.

Synthesis of Bi_2Te_3-Au/Bi_2Te_3@BSA (BTAB/BTB): 6 mg BTA/BT was dispersed in water, then 0.5 mL BSA aqueous solution (36 mg/mL) was dropwise added and stirred for 1h at room temperature. Material was stored in water.

20 μL of solution was drop-cast onto a carbon-coated film, air-dried, and subsequently subjected to TEM for morphological analysis. Materials were freeze-dried for testing (XPS, FTIR, XRD and UV-VIS-NIR).

Thermogravimetric analysis (TGA)

10 mg of the material was added into a crucible and then placed it in a thermal simultaneous analyzer. (The heating rate was 10°C/min, final temperature was 800°C, sampling interval was 1000 ms.)

Detection of ROS generation

ROS generation was detected by DCFH probe. 0.2 mg BT/BTA were dispersed in 2 mL 7.4 PBS solution with 0.2 mL DCFH working solution. The mixture alternately cycled between water bath at 25 °C and 50 °C, followed by fluorescence analysis of the supernatant. The excitation wavelength was set at 488 nm with a detection range of 500-600 nm. In H_2O_2 groups, the addition of H_2O_2 (100 mM) was performed before

water bathing.

Detection of •OH

0.2 mg BT/BTA were dispersed in 2 mL Methylene Blue (MB) aqueous solution with addition of 20 μL H_2O_2 (100 mM). The mixture was then heating and cooling by water bath. The absorbance of supernatant at wavelengths between 400-800 nm was detected by UV spectrophotometer. Using 5,5-dimethyl-1-pyrroline N-oxide (DMPO) as a spin trap, the generation of •OH was further detected via Electron Spin Resonance (ESR) spectroscopy. The heated BT/BTA NP PBS solution was mixed with DMPO, which was then transferred into a quartz capillary tube for testing and recording using an ESR spectrometer.

Detection of $\bullet O_2^-$

0.2 mg BT/BTA was dispersed in 2 mL 7.4 PBS with addition of 20 μL XTT aqueous solution (7.5 mg/mL). The mixture was then heating and cooling by water bath. The absorbance of supernatant at wavelengths between 400-600 nm was detected by UV spectrophotometer.

Detection of GSH consumption

DTNB was used to detect the consumption of GSH. A certain amount of materials was dispersed in GSH aqueous solution (0.5 mg/mL). The mixture was then cycled between water baths at 25°C and 50°C for different times. The supernatant was taken and added with DNTB for ultraviolet absorption testing.

Electrochemical Measurements

Electrochemical performance of material was tested on an electrochemical workstation. A working electrode was prepared by dropping 100 μL of the sample onto an ITO glass, and control group was blank ITO glass. The experimental setup included Ag/AgCl reference electrodes and platinum electrodes. The cooling and heating temperature were 0 °C and 65 °C respectively. Electrolyte solution was Na_2SO_4 (0.5

M).

Transient Absorption (TA)

1 mg BT and BTA were dispersed in 1 mL water for TA. Pump wavelength was 400 nm. Number of scan was 3.

Density Functional Theory (DFT) calculations

In this work, the crystal structure of bismuth antimonide(Bi_2Te_3) used for calculations was retrieved from Ref. [1]. A (2×2×1) supercell was constructed by expanding the primitive cell, followed by cleaving the bismuth antimonide crystal along the (001) plane. A 15 Å vacuum layer was then introduced to simulate the surface environment. All first-principles calculations based on spin-polarized density functional theory (DFT) were performed using VASP. For the purposes of these computations, the VASPKIT code [2] was utilized to generate key input files. The projector augmented wave (PAW) method was adopted to describe the ion–electron interactions, while the PBE functional, as formulated within the generalized gradient approximation (GGA), was selected to treat the electronic exchange–correlation energy. A plane-wave cutoff energy of 400 eV was set for the expansion of the valence electron wavefunctions. Convergence was deemed achieved when the total energy change fell below 10^{-6} eV and the maximum residual force on each atom was reduced to less than 0.02 eV/Å. The procedure of Bader charge analysis was performed with reference to Ref. [3-5].

The adsorption energy (E_{ad}) of the adsorbate at the sites in Bi_2Te_3 was calculated as follows:

$$E_{ad} = E_{slab+ads} - E_{slab} - E_{ads}$$

Where $E_{slab+ads}$, E_{slab} and E_{ads} denote the surface energy of the substrate with adsorbed adsorbate, the surface energy of the pristine substrate, and the surface energy of the adsorbate, respectively.

However, when the adsorbate is a charged molecule (e.g., the superoxide anion), a correction to its adsorption energy is required [6]. The modified calculation formula is

given below:

$$E_{ad} = E^{-}_{slab+ads} - E_{slab} - E^{0}_{ads} + q\mu_e$$

Where $E^{-}_{slab+ads}$ represents the surface energy of the system after adsorption of the charged molecule, E^{0}_{ads} denotes the surface energy of the original neutral molecule, q and μ_e corresponds to the charge amount of the adsorbate and Fermi level of the metal substrate.

Cytotoxicity assessment

Cytotoxicity of materials was tested by MTT. 0.1 mL of medium containing 10^4 cells was seeded into each well of a 96-well plate and incubated for 24 h. Then BTAB of different concentration were incubated with H22 and L929 overnight. Then 20 μL MTT was added. After 4 h, removing the supernatant and adding 200 μL DMSO. Centrifuging it and drawing 70 μL supernatant from it. Absorbance of 492 nm was measured to determine the cytotoxicity of material.

Tumor Cell Inhibition Assessment

1 mL of medium containing 10^5 cells into each well of a 6-well plate and incubated for 6 h, which was randomly divided into six groups. control group (G1), MW group (G2), BTB group (G3), BTB + MW group (G4), BTAB group (G5), BTAB + MW group (G6) (BTB and BTAB group with concentration of 50 μg/mL, MW group with 5 min MW irradiation of 2 W/cm^2). After incubating overnight, MTT was performed to assess the cell viability of each group. In addition, the Calcein-AM/PI was also used to assess intracellular anti-tumor efficiency.

Intracellular ROS Assessment

1 mL of medium containing 10^5 cells was seeded into each well of a 6-well plate and incubated for 6 h, which was randomly divided into six groups. Control group (G1), MW group (G2), BTB group (G3), BTB + MW group (G4), BTAB group (G5), BTAB + MW group (G6) (BTB and BTAB group with concentration of 50 μg/mL, MW group

with 5 min MW irradiation of 2 W/cm^2). 1 mL DCFH-DA probe solution (10 μm) incubated with cells for 30 min, then washing the cell pellet three times by PBS. The fluoresce intensity was observed under the fluorescence microscope.

Mitochondrial Membrane Potential Assessment

1 mL of medium containing 10^5 cells was seeded into each well of a 6-well plate and incubated for 6 h, which was randomly divided into six groups. Control group (G1), MW group (G2), BTB group (G3), BTB + MW group (G4), BTAB group (G5), BTAB + MW group (G6) (BTB and BTAB group with concentration of 50 μg/mL, MW group with 5 min MW irradiation of 2 W/cm^2). 1 mL JC-1 working solution probe was incubated with cells for 45 min after MW irradiation, then washing the cell pellet three times by PBS. The fluoresce intensity was observed under the fluorescence microscope.

Intracellular GSH consumption assessment

1 mL of medium containing 10^5 cells was seeded into each well of a 6-well plate, which was randomly divided into six groups. Control group (G1), MW group (G2), BTB group (G3), BTB + MW group (G4), BTAB group (G5), BTAB + MW group (G6) (BTB and BTAB group with concentration of 50 μg/mL, MW group with 5 min MW irradiation of 2 W/cm^2). The cell pellet was resuspended in 200 μL of cell lysis buffer and lysed for 30 minutes at room temperature. The supernatant was collected and mixed with 0.04 mL of DTNB aqueous solution. After reacting for 15 minutes, the intracellular GSH level was assessed by the absorbance at 412 nm.

In Vivo Therapeutic Effect Assessment

All animal experiments were approved by the Institutional Animal Care and Use Committee (IACUC) of the Technical Institute of Physics and Chemistry (TIPC) and conducted in accordance with their guidelines (IACUC-IPC-25011-002). Balb/c mice were purchased by Beijing Vital River Laboratory Animal Technology Co., Ltd. To assess the in vivo therapeutic efficacy, A primary tumor was established in Bald/c mice via subcutaneous injection of 1×10^6 H22 cells into the left axillary area. Then mice

were divided into five groups, including control group (G1), MW group (G2), BTB group + MW (G3), BTAB group (G4) and BTAB + MW group (G5). On day 0, 50 μL of material solution (10 mg/mL) was injected into intratumor, and the MW irradiation was conducted on tumors for 5 min. In summary, after anesthetizing and securing the mouse, the microwave source was placed against the tumor area. After radiating for a certain time, the source was briefly removed to record the temperature of tumor area, microwave frequency was 433 Mhz with power of 1.6 W/cm^2.Throughout the 14-day study, body weight and tumor volume were recorded daily. On day 14 of the treatment, the mice were euthanized, and their blood was collected for routine blood tests. For the detection of ROS in tumor tissues, the tumors were immediately excised after treatment, frozen-sectioned, and then stained using DCFH-DA.

Statistical Analysis

The quantitative data were presented as mean ± standard deviation (SD). The statistical analysis was calculated on one-way ANOVA test (*$p < 0.05$, **$p < 0.01$, ***$p < 0.001$ and ****$p < 0.0001$).

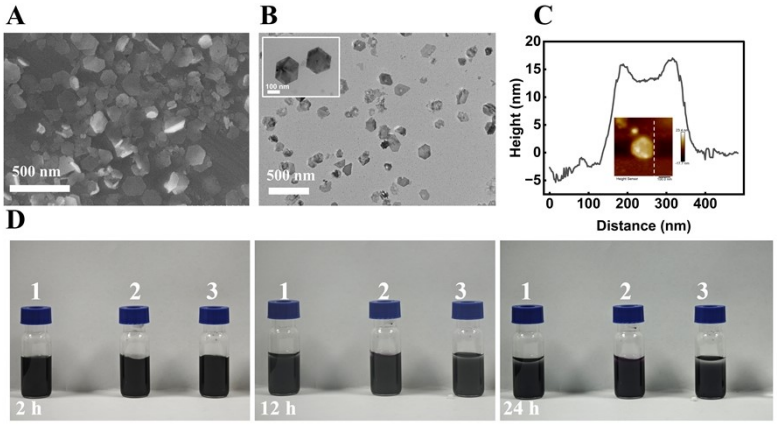

Fig. S1. (A) SEM, (B) TEM and (C) AFM image of BT. (D) BT dispersed in different solution for different time (1-water; 2-DMEM, 3-5% glucose solution).

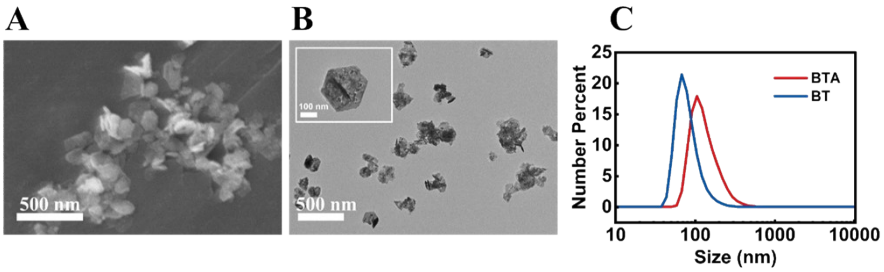

Fig. S2. (A) SEM image, (B) TEM image and (C) size distribution of BTA.

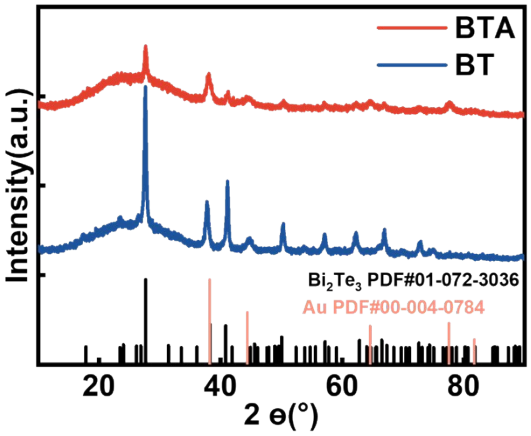

Fig. S3. XRD pattern of BT and BTA

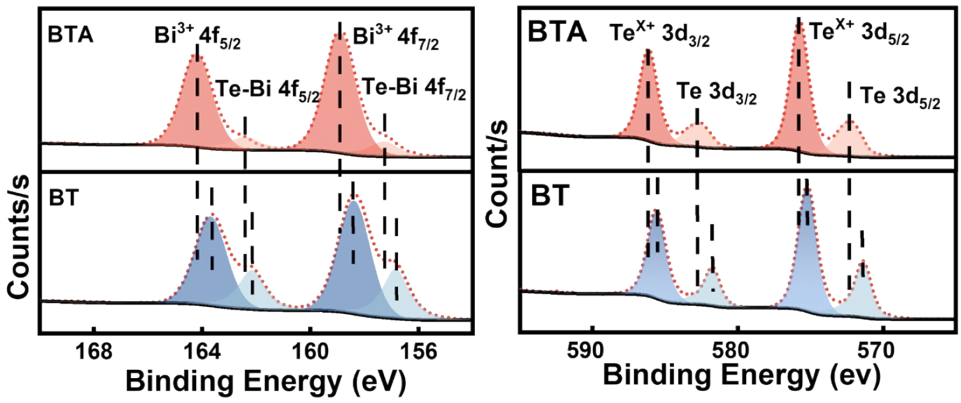

Fig. S4. Fine XPS of Bi and Te in BTA

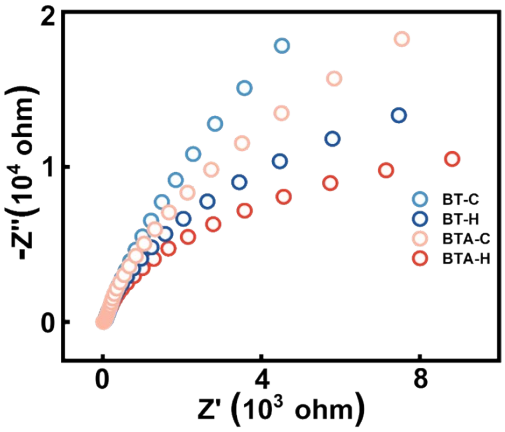

Fig. S5. EIS of BT and BTA at different condition

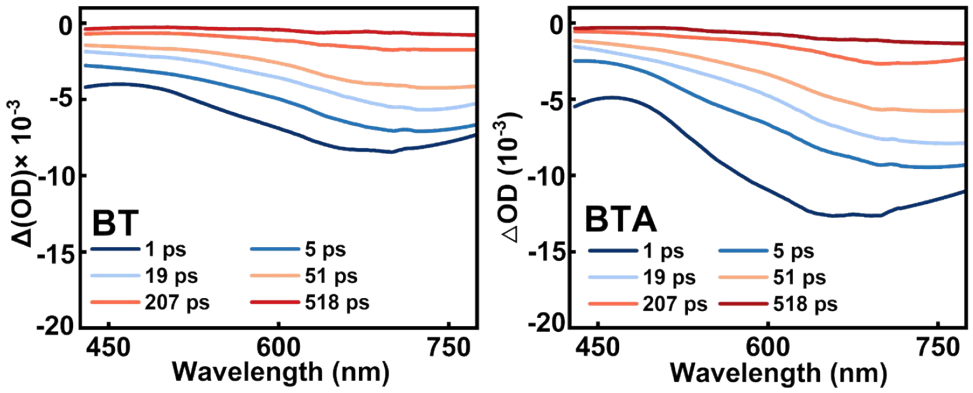

Fig. S6. TA spectra at different delay times of BT and BAT

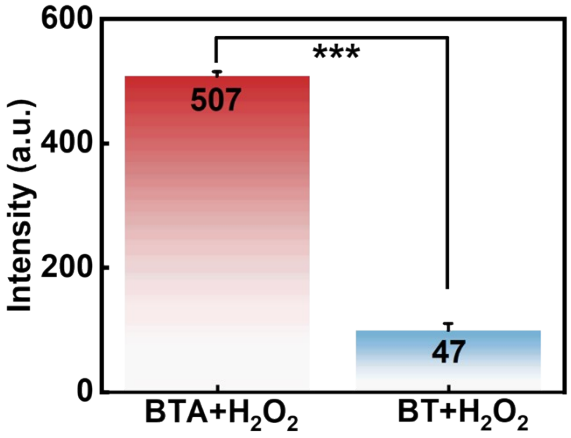

Fig. S7. The fluorescence intensity at 525 nm of different materials in the presence of hydrogen peroxide. (n=3)

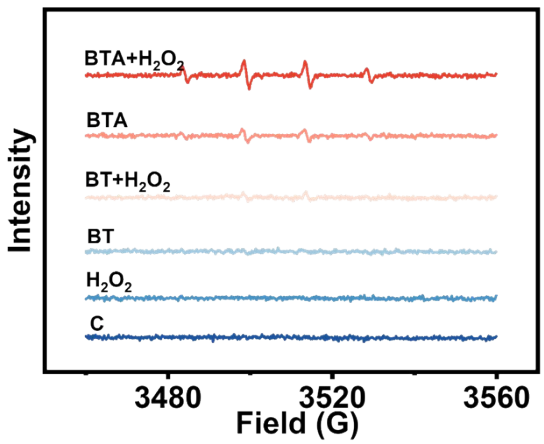

Fig. S8. ESR spectra of ·OH trapped by DMPO in different groups

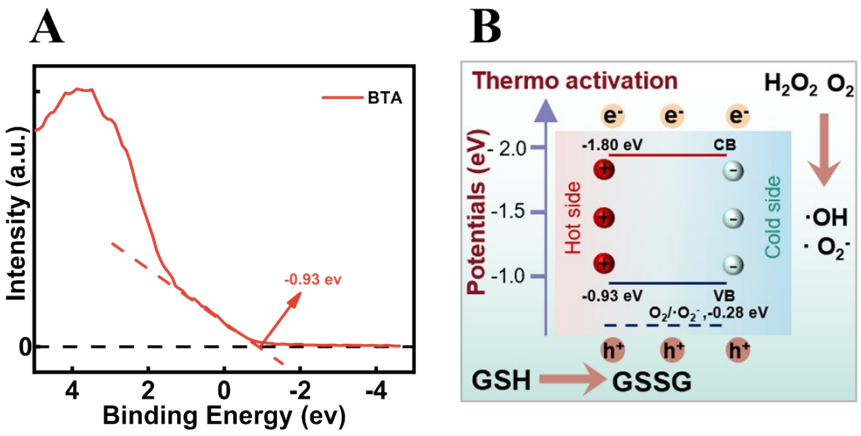

Fig. S9. (A) XPS valence band (VB) spectra and (B) band structure of BTA. (E_{CB}=E_{VB}-E_g)

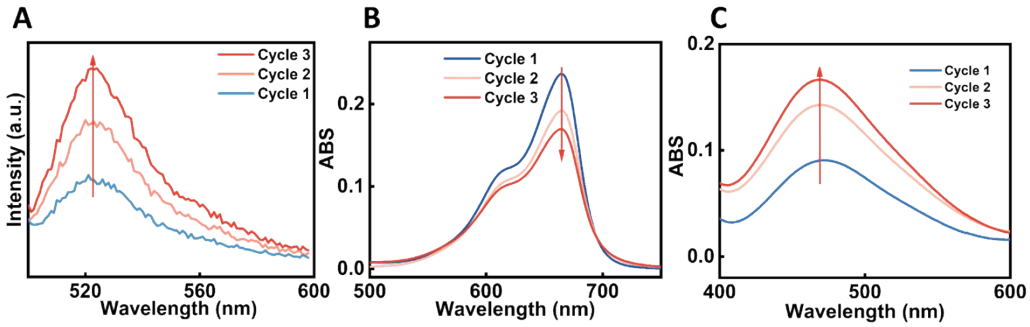

Fig. S10. Generation of (A) total ROS, (B) •OH and (C)•O_2^- of BTA after different heating/cooling cycles

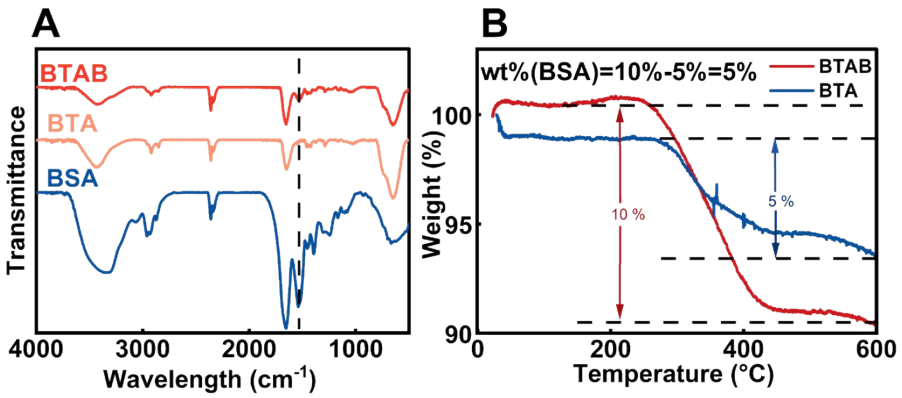

Fig. S11. (A) FTIR spectra and (B) TGA curve of BTAB

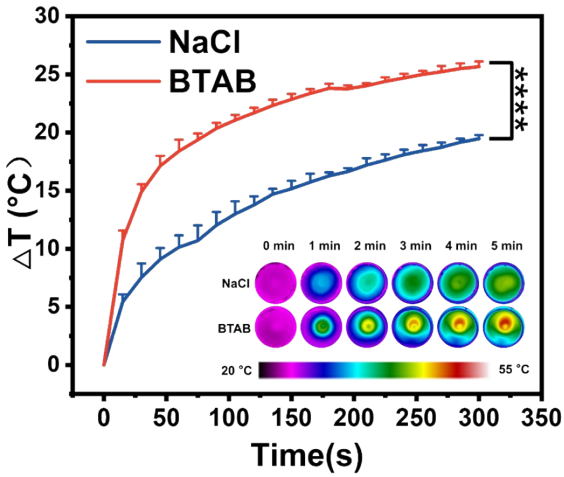

Fig. S12. Temperature rising curve of BAT under MW irradiation and corresponding infrared imaging. (*p < 0.05, **p < 0.01, ***p < 0.001 and ****p < 0.0001, n=3).

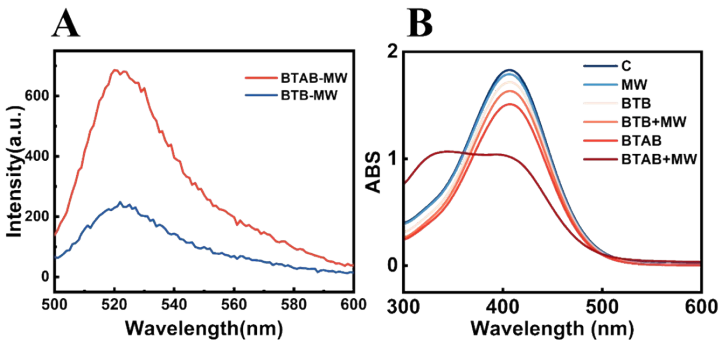

Fig. S13. (A) ROS generation and (B) GSH consumption of BTAB after MW irradiation

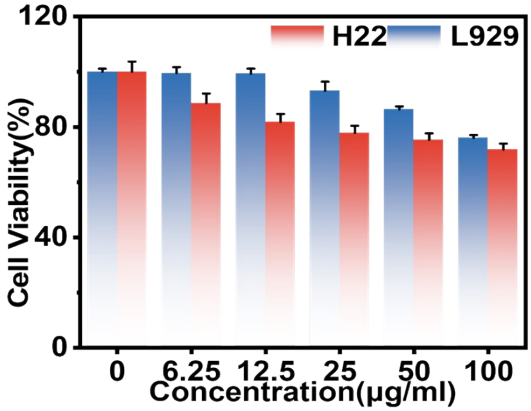

Fig. S14. Cytotoxicity assessment of BTAB to L929 and H22 cells

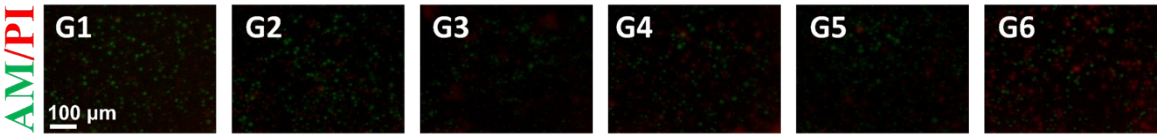

Fig. S15. CLSM images of H22 cells stained with AM/PI probe of different treatment groups

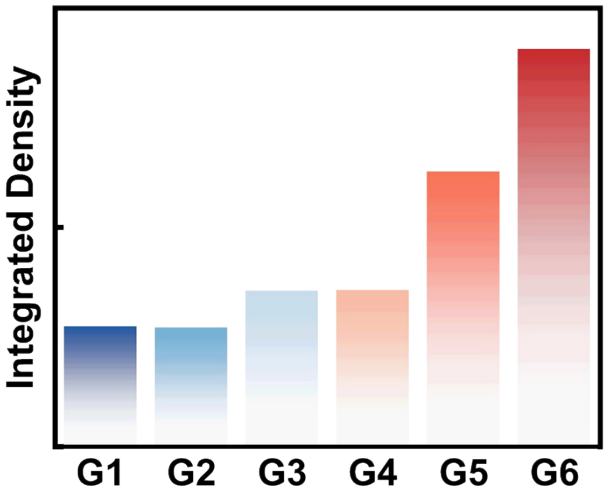

Fig. S16. Fluorescence quantitative analysis of intracellular ROS generation

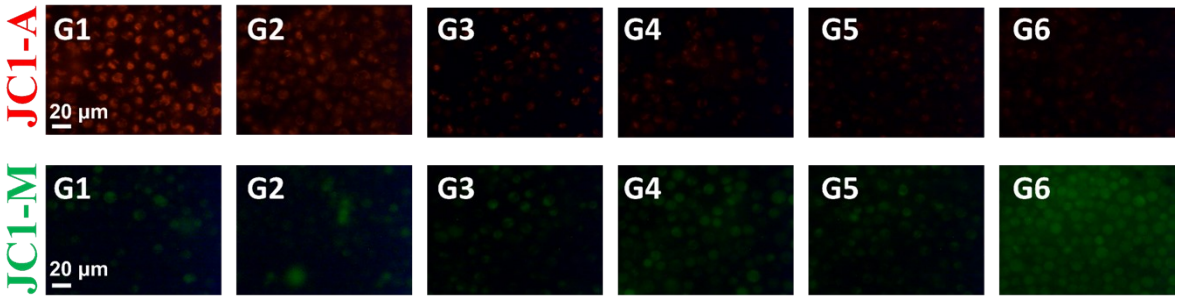

Fig. S17. CLSM images of H22 cells stained with JC-1 probe of different treatment groups

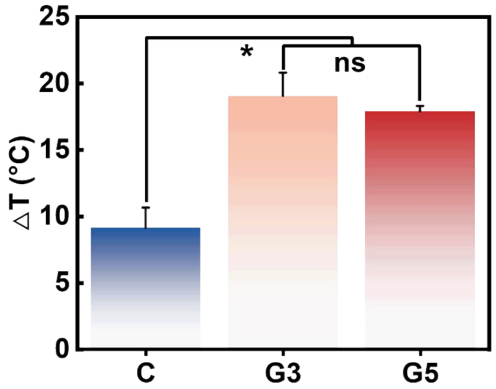

Fig. S18. The temperature change in tumor area after MW irradiation. (*p < 0.05, **p < 0.01, ***p < 0.001 and ****p < 0.0001, n=3).

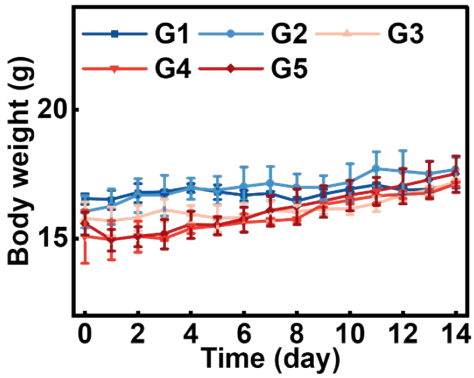

Fig. S19. Curves of body weight changes (n=3)

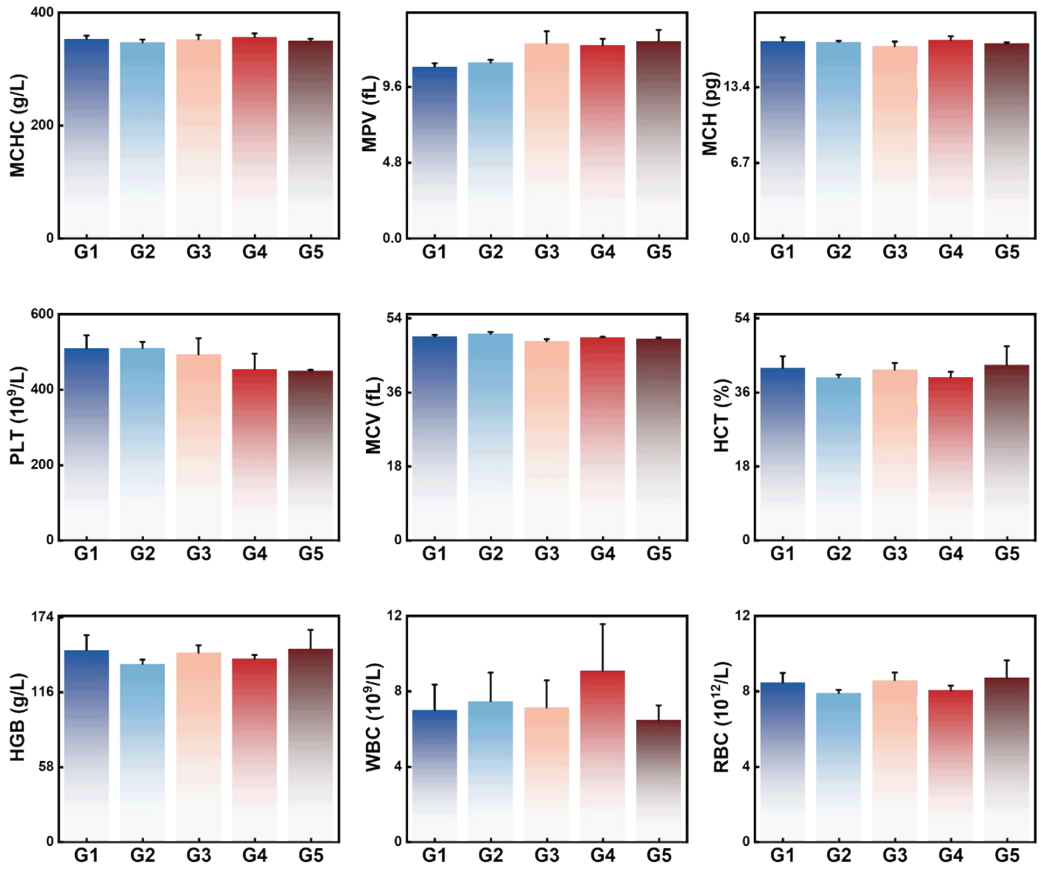

Fig. S20. Blood routine examination of different group. (n=3)

References

1 M. Yao, Y. Wang, X. Li, Y. Sheng, H. Huo, L. Xi, J. Yang and W. Zhang, *Sci. Data.*, 2021, **8**, 236.

2 V. Wang, N. Xu, J.-C. Liu, G. Tang and W.-T. Geng, *Comput. Phys. Commun.*, 2021, **267**, 108033.

3 W. Tang, E. Sanville and G. Henkelman, *J. Phys-condens. Mat.*, 2009, **21**, 084204.

4 E. Sanville, S. D. Kenny, R. Smith and G. Henkelman, *J. Comput. Chem.*, 2007, **28**, 899-908.

5 G. Henkelman, A. Arnaldsson and H. Jónsson, *Comput. Mater. Sci.*, 2006, **36**, 354-360.

6 C. Freysoldt, B. Grabowski, T. Hickel, J. Neugebauer, G. Kresse, A. Janotti and C. G. Van de Walle, *Rev. Mod. Phys*, 2014, **86**, 253-305.